On the bow shock θ_{Bn} dependence of upstream 70 keV to 2 MeV ion fluxes

K. Meziane,[1] A. J. Hull,[2] A. M. Hamza,[1] and R. P. Lin[2]

Received 26 February 2001; revised 20 January 2002; accepted 20 January 2002; published 19 September 2002.

[1] We present a statistical study of 216 energetic ion events observed just upstream of Earth's bow shock by the Wind spacecraft. The ions that compose this database range in energy from 27 keV to 2 MeV. Of particular interest is the effect of shock geometry on the properties of the energetic ions. Our approach is different from previous studies in that we only include upstream ion events associated with a local bow shock crossing. In this way we determine the shock geometry locally, rather than from extrapolations of remote upstream observations to a model shock source location, providing a better quantitative determination of the properties of the energetic ions in relation to shock geometry. Under typical interplanetary conditions in the absence of a preexisting population of ambient energetic ions ($E \geq 50$ keV), we find that the ion energy spectrum is characterized by an energy cutoff at $\sim$200–330 keV. Neither the energy cutoff nor the energetic ion spectrum show any dependence on shock geometry as measured by the angle between the shock normal and magnetic field θ_{Bn}. However, when an ambient population of energetic particles is present in the interplanetary medium, ion flux levels measured just upstream of the terrestrial shock reach a minimum near $\theta_{Bn} \sim 45°$ irrespective of energy. The energy spectrum spans up to $\sim$2 MeV. Moreover, ions with energies $E \geq 550$ keV are observed only at $\theta_{Bn} \geq 45°$. The flux levels of these more energetic ions increase, in an average sense, with increasing values of θ_{Bn}. *Lee*'s [1982] self-consistent theory of ion diffusive shock acceleration appears to explain the energetic ion flux levels observed at $\theta_{Bn} \leq 40°$. Upstream energetic ions with energies $E \geq 550$ keV appear to be the result of shock drift acceleration. *INDEX TERMS:* 2116 Interplanetary Physics: Energetic particles, planetary; 2134 Interplanetary Physics: Interplanetary magnetic fields; 2154 Interplanetary Physics: Planetary bow shocks; 2164 Interplanetary Physics: Solar wind plasma; *KEYWORDS:* shock drift acceleration, corotating interaction regions, Fermi acceleration, shock-associated particle acceleration, interplanetary shocks, upstream energetic ions

Citation: Meziane, K., A. J. Hull, A. M. Hamza, and R. P. Lin, On the bow shock θ_{Bn} dependence of upstream 70 keV to 2 MeV ion fluxes, *J. Geophys. Res.*, *107*(A9), 1243, doi:10.1029/2001JA005012, 2002.

1. Introduction

[2] The properties of energetic ions generated at Earth's bow shock have been extensively studied over the past two decades [e.g., *Bonifazi and Moreno*, 1981; *Paschmann et al.*, 1981; *Ipavich et al.*, 1981; *Thomsen*, 1985; *Fuselier*, 1994; *Skoug et al.*, 1996; *Desai et al.*, 2000; *Freeman and Parks*, 2000]. The energetic ions have been observed to range in energy from $\sim$1 keV to few MeV [*Skoug et al.*, 1996]. Energetic ions emanating from the bow shock are identified via their occurrence on interplanetary magnetic field lines connected to the shock [*Lin et al.*, 1974; *Bonifazi and Moreno*, 1981]. Numerous observational studies suggest that the occurrence and detailed properties of upstream energetic ions strongly depend on shock geometry [*Scholer et al.*, 1980; *Bonifazi and Moreno*, 1981; *Gosling et al.*, 1982; *Mitchell and Roelof*, 1983]. Field-aligned ion beams with energies of few keV propagating upstream of the Earth's bow shock appear to originate from regions of the shock having θ_{Bn} between 35° and 75° [*Bonifazi and Moreno*, 1981], θ_{Bn} being the angle between the magnetic field vector and the local shock normal. The more recent study by *Meziane et al.* [1999] found evidence of nongyrotropic energetic protons with energies $\sim$2 MeV that appear to emanate from nearly perpendicular shock regions ($\theta_{Bn} \sim 90°$). Nearly isotropic ion distributions with energies extending up to but less than $\sim$300 keV are generally observed to be associated with turbulent quasi-parallel shock regions [*Lin et al.*, 1974; *Greenstadt et al.*, 1980; *Bonifazi and Moreno*, 1981].

[3] The statistical study by *Scholer et al.* [1980] was the first to explore the frequency of occurrence of upstream ions with energies >30 keV as a function of shock geometry using data from ISEE 1. The authors found that more than

[1]Physics Department, University of New Brunswick, Fredericton, New Brunswick, Canada.
[2]Space Sciences Laboratory, University of California, Berkeley, California, USA.

0148-0227/02/2001JA005012$09.00

50% of the events occurred for values of $\theta_{Bn} \leq 15°$, with few events occurring for values of $\theta_{Bn} \geq 45°$. These results were confirmed by *Mitchell and Roelof* [1983] using data registered by the EPE particle experiment on board of IMP 7 & 8 orbiting in a circular orbit at ~35 R_E from Earth. *Mitchell and Roelof* [1983] demonstrated that the probability of occurrence of upstream 50–200 keV ion events decreases with increasing θ_{Bn}. In both the ISEE and IMP 7 & 8 studies, the angle θ_{Bn} was computed using a bow shock model and assuming straight magnetic field lines, on average, between the shock and the spacecraft. Moreover, the study by Mitchell and Roelof included very few events in the vicinity of the bow shock. Although Mitchell and Roelof did not address the source of the observed energetic ions, their studies suggest that the ion acceleration process is a strong function of shock geometry.

[4] Various theoretical models have been proposed to explain the observed properties of energetic ions associated with collisionless shock waves. One model believed to be effective in energizing ions at collisionless shocks is the Shock Drift Acceleration (SDA) model. In this model, ions gain energy as they drift along the shock surface in the direction of the induced motional electric field. The SDA mechanism is strongly dependent upon the angle θ_{Bn}, being most effective in accelerating ions at quasi-perpendicular geometries. At quasi-parallel shock geometries, the SDA mechanism is less efficient than the curvature drift mechanism which predicts ions to lose energy [*Forman and Webb*, 1985]. Therefore, scatter-free shock acceleration can not explain the energetic ion flux enhancements observed at these geometries. One mechanism often invoked to explain the energization of ions at quasi-parallel shocks is the first-order Fermi process. In this process ions gain energy by multiple traversals of a turbulent shock layer [*Forman and Webb*, 1985]. The Fermi mechanism can efficiently accelerate ions up to ~200–300 keV [*Terasawa*, 1979b, 1981; *Lee*, 1982; *Scholer*, 1990]. In the case of Earth's bow shock, ions can be trapped between the magnetic turbulence associated with the quasi-parallel shock and the shock itself, and via the Fermi process could gain a significant amount of energy.

[5] Another scenario put forward in order to explain the observed properties of upstream energetic ions regards the leakage model. This hypothesis assumes that the acceleration takes place somewhere in the magnetosphere, and then upflowing ions find their way to escape in the solar wind [*Sarris et al.*, 1987]. *Edmiston et al.* [1982] suggested that the suprathermal ions, with energies ranging from 1 to 10 keV, are the result of a magnetosheath source that escapes into the upstream plasma. *Edmiston et al.* [1982] demonstrated using a leakage model that significant fluxes may be generated for $\theta_{Bn} \leq 45°$.

[6] Despite considerable attention, the mechanism or mechanisms that determine the detailed properties of the energetic ion flux spectrum observed just upstream of Earth's bow shock are still unclear. In this paper, we present the results of a detailed statistical study of the relation between shock geometry and the flux levels of ions with energies in the range of 27 keV to 2 MeV as observed by the Wind-3DP experiment. By focusing our attention on the statistical properties of the flux levels, we are better able to evaluate the accuracy of various theoretical models proposed to explain the signatures and hence the source of the upstream energetic ions. Our study is complimentary to that performed by *Mitchell and Roelof* [1983] even though we use a different approach. Namely, our study focuses on the detailed properties of the flux spectrum of upstream propagating energetic ions observed just upstream of terrestrial bow shock crossings. A major advantage of our approach is that the shock geometry is determined locally, rather than from extrapolations of remote upstream observations to a model shock source location. Moreover, the Wind 3-Dimensional (3D) Plasma and Energetic Particle experiment [*Lin*, 1995] provides complete coverage of the ion distribution function, and hence more accurately determined energetic ion flux levels. In this way our analysis provides a better assessment of the properties of the energetic flux levels in relation to shock geometry and hence provides important constraints on models/mechanisms proposed to explain the energetic ions observed in the vicinity of Earth's bow shock. In section 2, we discuss our selection criteria and our analysis method. Example events are discussed in section 3 and results of our analysis of 216 upstream propagating ion events measured near Earth's bow shock are given in section 4. The trends found in the data are discussed in the context of theoretical models in section 5 and conclusions are given in section 6.

2. Data Selection and Method of Analysis

[7] The present study is based on measurements of upstream energetic ion fluxes by the Wind-3D Plasma and Energetic Particle experiment [*Lin et al.*, 1995]. Suprathermal ions, with energies $E \leq 30$ keV, are detected by an analyzer with a high geometrical factor (PESA-H). Ions with energies ranging from 70 keV up to ~4 MeV are detected by three pairs of double-ended telescopes (Solid State Telescope or SSTs). The pairs of detectors provide full three dimensional coverage with good angular resolution; the energy resolution is $\Delta E/E \sim 0.2$. We use a 48-second time resolution (16 spin periods) for ions with energies up to 30 keV. The time resolution for higher energies varies between 6 s (for 70 keV) and 48 s (for 4 MeV). The plasma data used in this paper are taken from the PESA-Low analyzer which monitors the solar wind. The magnetic field data are obtained from the Magnetic Field Investigation experiment [*Lepping et al.*, 1995].

2.1. Selected Ion Fluxes

[8] It is important to emphasize that only energetic ion events that occurred just upstream of an Earth bow shock crossing were included in our database. Figure 1 shows the locations (indicated by pluses) of the Wind satellite bow shock crossings between 30 November 1994 and 25 January 2000 associated with the 254 energetic ion events that make up our data set. The solid curve represents a paraboloid shape of the nominal bow shock position as predicted by the MHD model of *Cairns et al.* [1995]. We see that some crossings occurred near the flanks of the bow shock at $X_{GSE} \sim -50\ R_E$. Shock associated energetic ion events are identified by their connection to Earth's bow shock. Two independent methods were used to establish which regions encountered by Wind were magnetically connected and which were not connected to Earth's bow shock. The first method is to look for enhancements in the more or less constant flux levels of

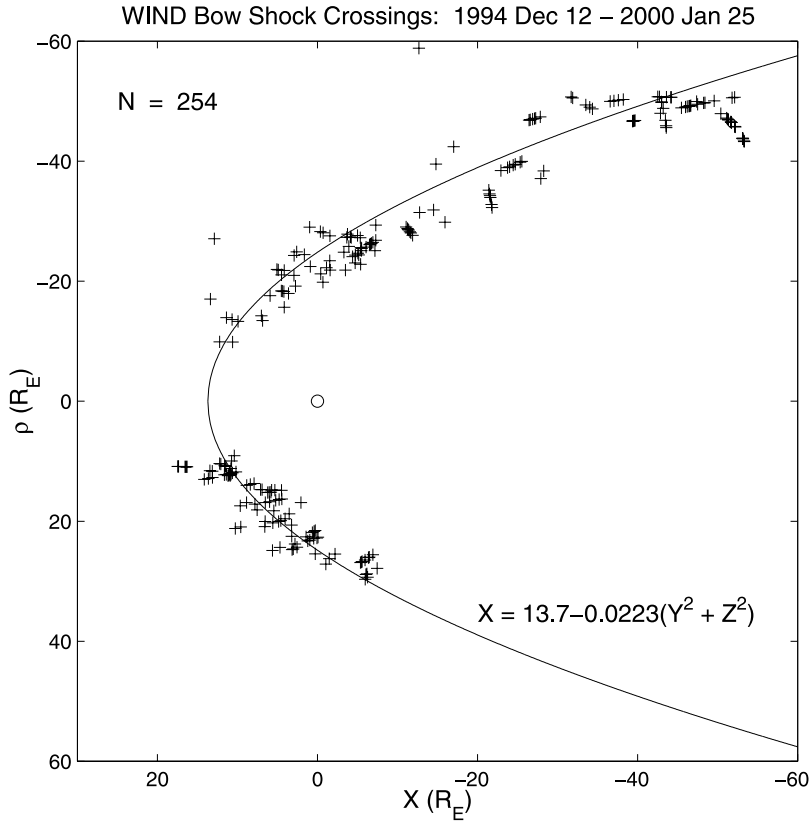

Figure 1. Locations of the Wind satellite bow shock crossings from 12 December 1994 to 25 January 2000. The continuous curve corresponds to the nominal bow shock.

ions with 1–30 keV energies measured by PESA-H. Regions that are magnetically connected to the shock have ion flux levels in the 1–30 keV energy range that are enhanced relative to the undisturbed solar wind levels. These enhancements are easy to identify in the data, providing a reliable determination of magnetic connection to the bow shock. The second method is to determine whether a straight line extrapolation of the magnetic field measured at the spacecraft intersects a model bow shock. This method has been used by many authors [e.g., *Lin et al.*, 1974; *Bonifazi and Moreno*, 1981; *Mitchell and Roelof*, 1983] and is generally reliable provided the spacecraft is relatively close to the bow shock. In this paper, we used the model developed by *Cairns et al.* [1995] to determine magnetic connection via the second method. We compared the results of both methods and found them to be in agreement.

[9] We are interested in determining the relationship between flux levels of upstream propagating ions and shock geometry, in addition to making quantitative assessments of shock acceleration models. Thus, only events associated with ions moving away from the shock were included in our study. For the purpose of comparison with shock acceleration models, we used omnidirectional fluxes corrected for background counts associated with cosmic rays, sunlight contamination, instrumental noise, and, if present, ambient energetic ions. The background count levels for each energy step and angular bin were determined from measurements sampled in interplanetary regions not magnetically connected to the terrestrial shock as close to each ion event as possible. The estimated background count levels were subtracted from counts accumulated in the same energy and the same angular bins pertaining to a given ion event, prior to ascertaining the omnidirectional flux enhancements relative to background for each energy step. Only count differences greater than three standard deviations were considered to have nonzero counts. We use 3σ criterion because of the low statistics of measurement for $\geq$70 keV ions.

2.2. Determination of θ_{Bn}

[10] A precise determination of the shock normal is not an easy task, because of the nature of the shock structure. Different methods have been used depending on the availability of data and conditions. Perhaps the most reliable method of determining the shock normal and hence θ_{Bn} is the least squares method developed by *Viñas and Scudder* [1986], which is based on a subset of the Rankine-Hugoniot conservation relations. This method requires reliable determinations of electron and/or ion moments, in addition to magnetic field data. Problems with spacecraft potential estimates, essential for accurate determinations of electron moments, coupled with saturation problems, and the dramatic changes in ions which requires measurements from two different detectors for accurate downstream ion moments precludes routine application of the method developed by *Viñas and Scudder* [1986] at this time and is therefore left for future work.

[11] In this study, we applied the minimum variance (MV) method to spin-period-averaged magnetic field data to determine the local shock geometry [*Sonnerup and Cahill*, 1967]. This method relies on the magnetic field

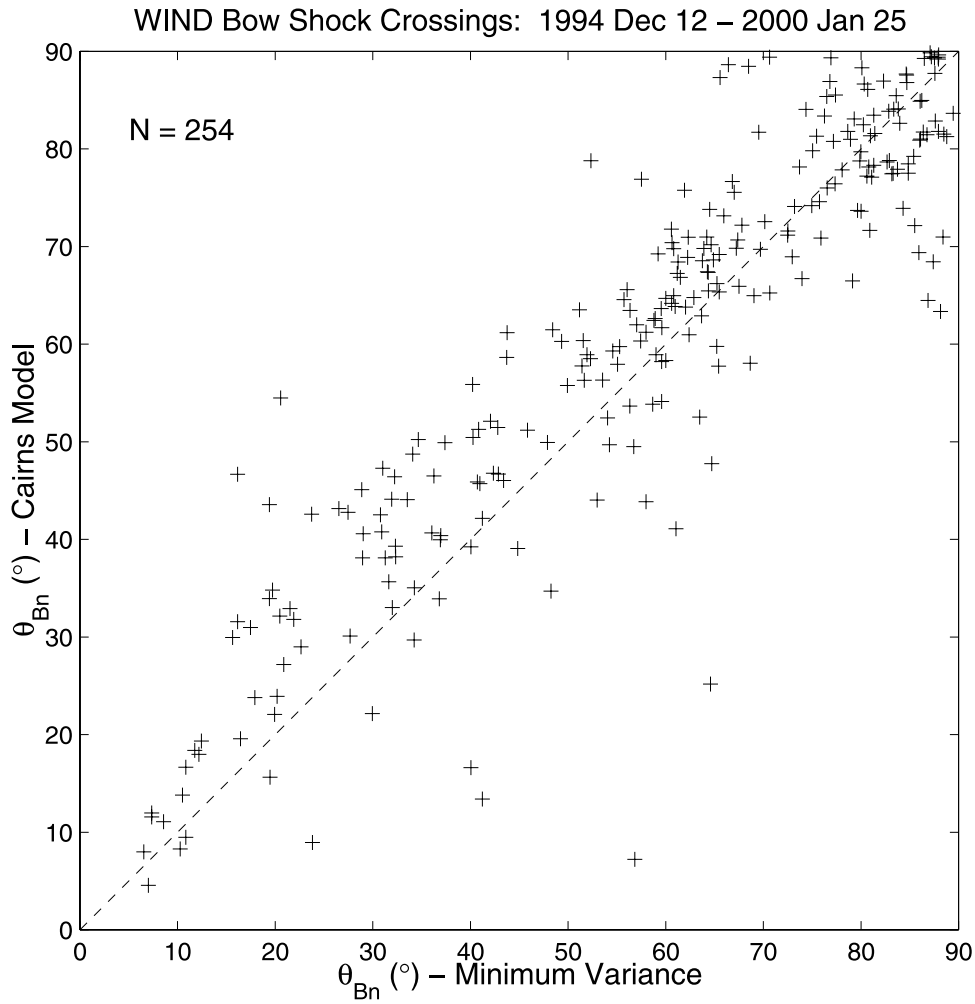

Figure 2. Comparison between θ_{Bn} computed using the minimum variance analysis and *Cairns et al.*'s [1995] MHD model.

data only and is based on the constancy of the normal component of the magnetic field through the shock. The shock normal is determined by finding the eigenvalues and associated eigenvectors of the covariance matrix defined by the magnetic fields sampled over some finite time encompassing the shock. The eigenvector associated with the minimum eigenvalue represents the shock normal direction. The MV method yields reliable normal determinations provided the ratio between the intermediate and minimum eigenvalue $\lambda_2/\lambda_1 \gg 1$. It is important to note that the presence of electromagnetic waves with wave vectors not aligned along the shock normal could influence the minimum variance determination of the shock normal.

[12] The uncertainty in the shock normal direction is related to the uncertainty in our knowledge of the shock macroscopic magnetic field direction in the presence of fluctuations, which can be approximated by $\tan \delta\theta \propto \delta B/B_0$, where δB is the fluctuation in the magnetic field associated with the wave and B_0 is the background magnetic field. One type of electromagnetic disturbance commonly observed at shocks is the whistler mode. According to *Zhang et al.* [1999], the most intense whistlers encountered by Geotail at the bow shock were typically found to have $\delta B/B_0 \sim 0.1$, which would suggest an angular uncertainty of $\delta\theta \sim 6°$. Thus in general minimum variance analysis should provide a good estimate of the shock normal and hence θ_{Bn} provided $\delta B/B_0$ is sufficiently small. Minimum variance analysis applied to shock layers containing magnetic fluctuations with amplitudes comparable to the background shock field structure could yield inaccurate results. In general, averaging over the spin period effectively removes effects associated with upstream propagating whistlers and the like from the data set, but may not adequately remove ULF wave effects (if present), which are often observed at more parallel shock regions. Thus, as a cross check of the minimum variance determinations, we use the model developed by *Cairns et al.* [1995] to provide independent estimates of θ_{Bn} for the events that make up our database. This empirical model is based on fits to a statistical database of shock crossings, and given the solar wind ram pressure and the fast magnetosonic Mach number provides estimates of the shock normal and hence θ_{Bn}, which are reliable in an average sense.

[13] Figure 2 compares the minimum variance estimates of θ_{Bn} with the model determinations of θ_{Bn} for 254 candidate events. Figure 2 clearly shows that, for the most part, the results of the two methods are in good agreement, with the best fit slope being .82 ± 0.15 and the linear

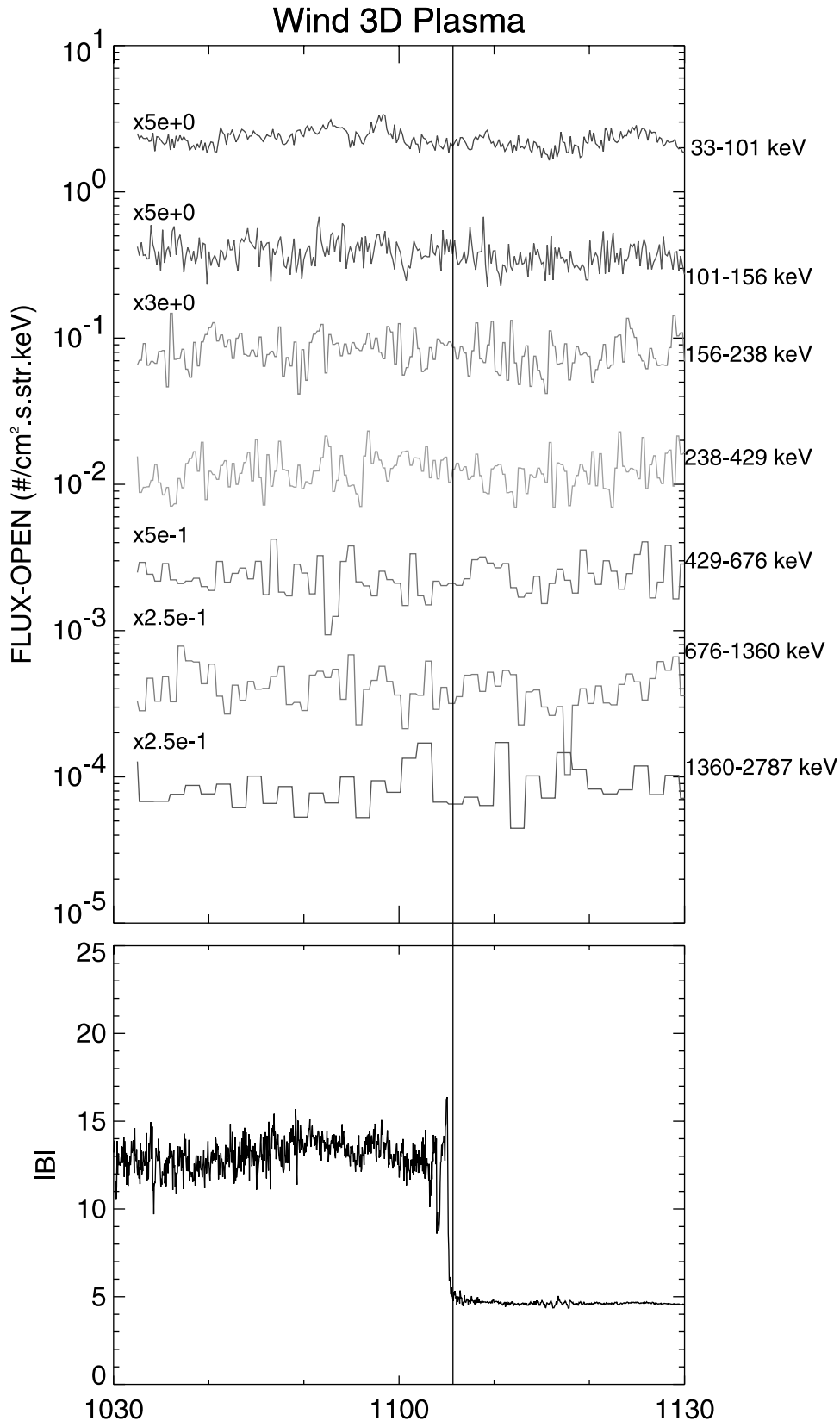

Figure 3. Energetic ion fluxes (top frame) and interplanetary magnetic field magnitude (bottom panel) registered on 3 January 1999 between 1030 and 1130 UT. For clarity the flux for each energy channel has been multiplied by scaling factors adjacent to each trace.

correlation coefficient found to be .93. The distribution of the difference between the two results is Gaussian distributed about zero with a dispersion of $\sim$11°. There are some candidate events where the θ_{Bn} results were in poor agreement. Thus, for the purposes of this study, only those events which had $\leq$11° differences in the θ_{Bn} values determined via the two different methods were included in our data set. A total 216 out of 254 candidate events satisfied this selection criteria. The best fit slope using only the remaining filtered events is .89 ± 0.16, with a linear correlation coefficient equal to .94.

3. Case Examples

[14] In this section we present examples of the different classes of events that make up our statistical database. The first example is given in Figure 3, which shows observations registered on 3 January 1999 for the time interval 1030–1130 UT. The top panel shows the differential ion flux for different energy channels registered by the SST-OPEN telescope and the bottom panel gives the magnetic field intensity. Wind crossed the bow shock at 1105:45 UT as indicated by the sharp increase in the magnetic field magnitude. This crossing is observed during typical solar wind conditions, with the solar wind velocity $V_{SW} \sim$ 370 km/s, solar wind density $n_{SW} \sim 4\ cm^{-3}$, and the plasma $\beta \sim 0.6$. No ambient population of energetic ions with energies $E \geq$ 50 keV was observed in the interplanetary medium. We mention that the entire upstream region is connected to the bow shock. As a reference, Figure 4 indicates the location of Wind at the shock crossing. The solid curve delineates the bow shock cross section that contains the solar wind direction, *X*, the magnetic field vector, and the Wind's position at the time of the shock crossing. The local shock normal **n** as well as the magnetic field vector **B** are also indicated in Figure 4. The angle θ_{Bn}^{MV} determined via the minimum variance method (see subsection 2.2) was found to be 61°, which is in reasonable agreement with the value $\theta_{Bn}^{BS} = 70°$ obtained by using bow shock model method. These values of θ_{Bn} demonstrate that the shock crossing is of quasi-perpendicular geometry. Such shocks tend to be laminar in structure and are nearly free of magnetic turbulence upstream of the shock of sufficient amplitude and low enough frequency to affect the ion dynamics. In this example, we see no energetic ion intensity enhancements associated with the shock crossing. The ion flux for each energy channel is on average constant throughout the shock layer proper.

[15] A second type of event included in this study is illustrated in Figure 5, which shows data from Wind on 1 October 1997, between 1530 and 1630 UT. Wind first encounters the bow shock at 1555:16 UT. In this example, the magnetic field vector is directed into the shock toward the downstream side, as illustrated in Figure 6a. This event is also observed during nearly typical interplanetary conditions ($V_{SW} \sim$ 480 km/s, $n_{SW} \sim 7\ cm^{-3}$ and $\beta \sim 0.5$). The shock is of quasi-perpendicular geometry, with $\theta_{Bn}^{MV} = 89°$, which is comparable to the value obtained from the bow shock model method. No ambient energetic ions with $E \geq$ 50 keV were observed in adjacent unconnected interplanetary regions. A sharp increase in the energetic ion flux is observed just upstream of the bow shock. The enhancement

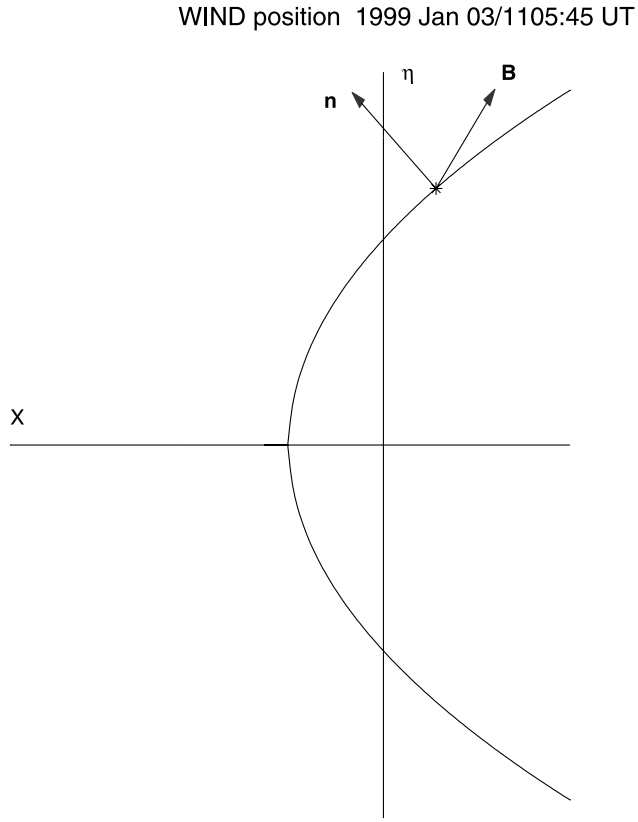

Figure 4. Shock geometry for the Wind satellite bow shock crossing on 3 January 1999 at 1105:45 UT.

in the ion flux levels persists even into the downstream side of the shock. To show that the energetic ions observed upstream are moving away from the shock, Figure 6b depicts the ion flux as a function of pitch angle, α, for E = 70, 128 and 198 keV measured at 1555:04–1555:10 UT. Given the orientation of the magnetic field for this event, values of $\alpha < 90°$ represent ions propagating toward the shock, while $\alpha > 90°$ represent ions moving further upstream away from the shock. The flux levels being significant for values of $\alpha > 90°$ in Figure 6b demonstrates that the ions measured just upstream of the shock are propagating upstream away form the shock. We also examined the ion fluxes as a function of α of ions measured just downstream of the terrestrial bow shock crossing at 1555:16 UT and found that the ions are moving toward the shock. Thus the ions observed upstream may be of two possible sources: (1) ions of magnetospheric origin or (2) ions with origins in the solar wind that traversed the curved bow shock into the downstream side and have subsequently leaked back into the upstream side of the shock.

[16] Another type of event observed during quiet solar wind conditions is illustrated in Figure 7, which shows data from Wind on 1 October 1997, between 0900 and 0930 UT. In this example, Wind observed an increase in ion fluxes at 33–429 keV energies within and just upstream of the shock ramp located at 0924:10 UT. Using *Cairns et al.*'s [1995] bow shock model, we found $\theta_{Bn}^{BS} = 71°$, which is consistent with the minimum variance analysis result of $\theta_{Bn}^{MV} = 77°$. The local shock normal **n** as well as the magnetic field

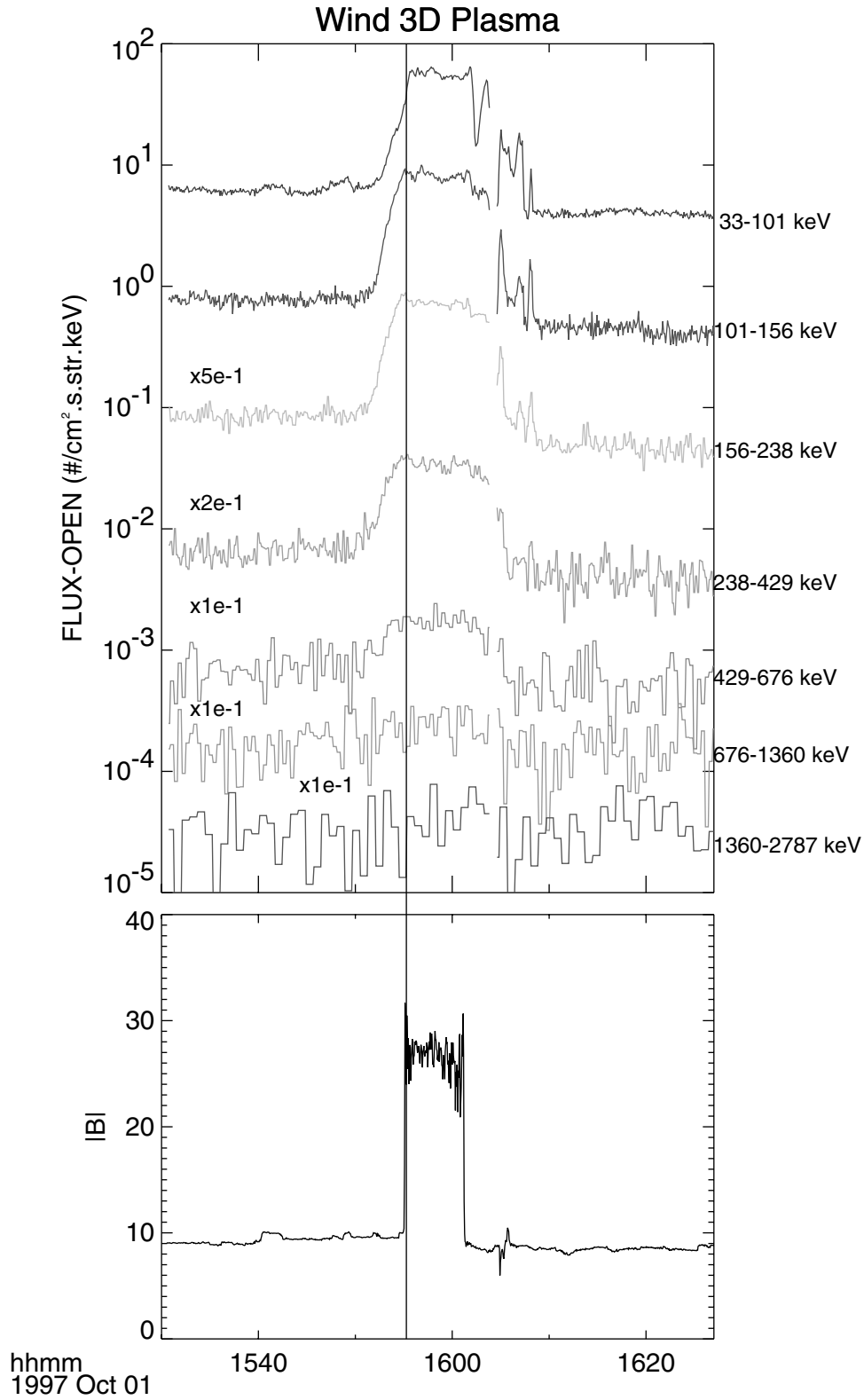

Figure 5. Same as in Figure 3 for 1 October 1997 between 1530 and 1630 UT.

vector **B** at the crossing location are illustrated on Figure 8a. In this example the magnetic field vector points into the shock. The ion pitch angle distribution measured at 0624:14–20 UT is shown on Figure 8b. With values of $\alpha > 90°$ representing upstream propagation, Figure 8b clearly indicates that the energetic ions observed just upstream are moving away from the shock.

[17] The three examples discussed above were observed during typical interplanetary conditions in the absence of any ambient energetic particles. However, events associated with

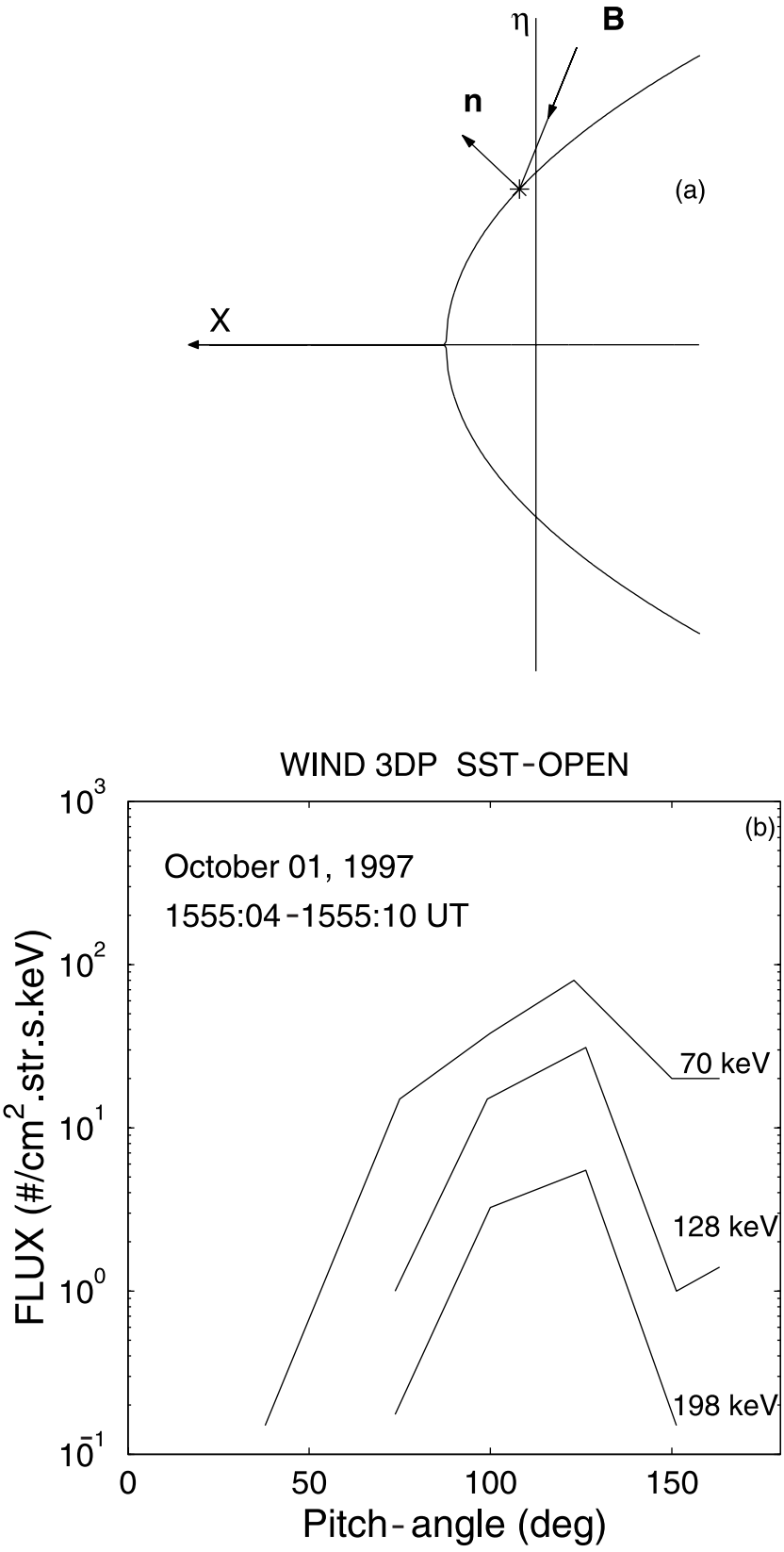

Figure 6. Top panel (a) indicates the shock geometry for the Wind bow shock crossing. Bottom panel (b) shows the particle pitch angle distribution for E = 70, 128 and 198 keV as registered just upstream of the bow shock on 1 October 1997 at 1555:04–1555:10 UT.

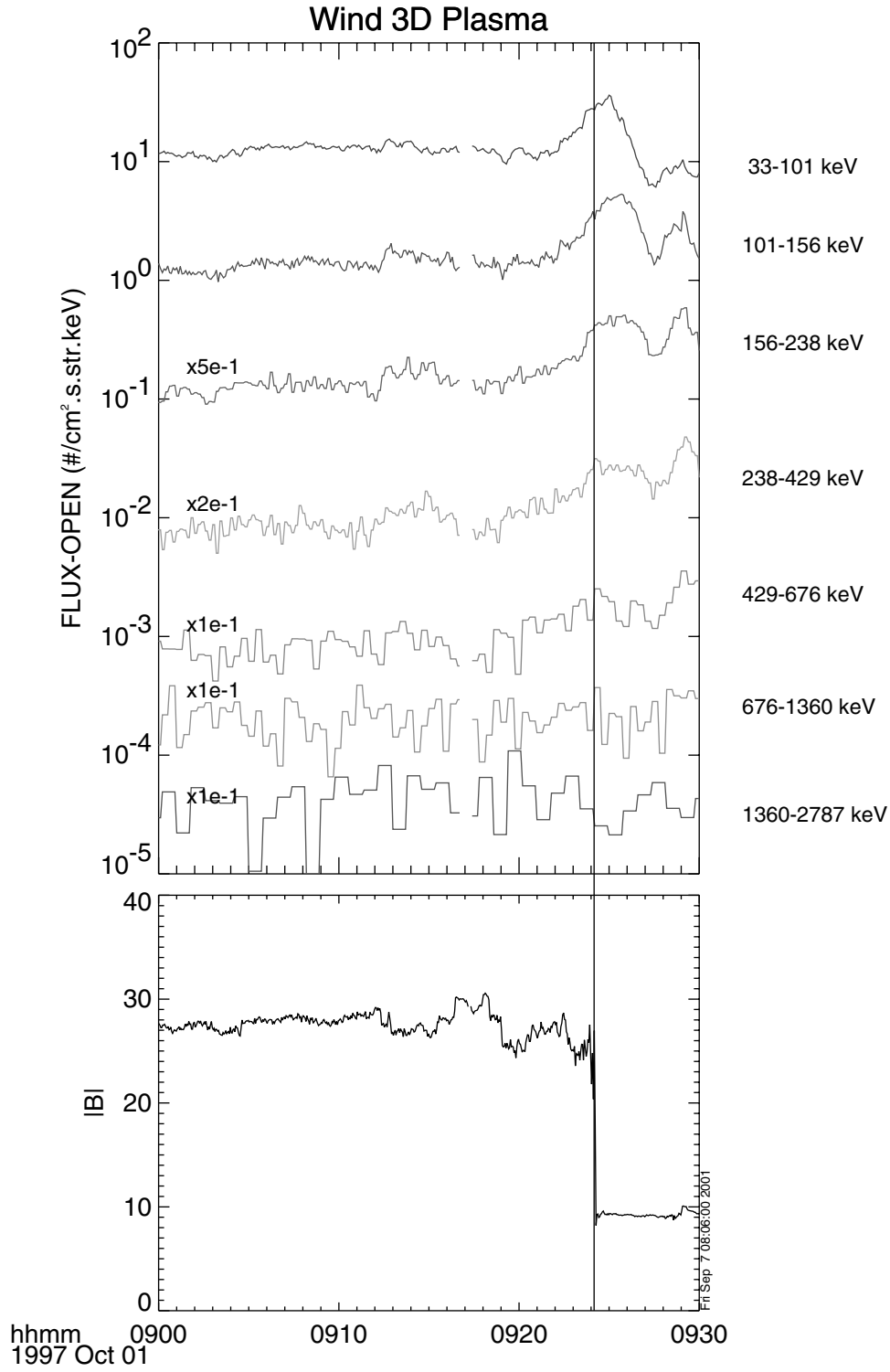

Figure 7. Same as in Figure 3 for 1 October 1997 between 9000 and 0930 UT.

a preexisting (ambient) population of energetic particles with $E \geq 50$ keV have also been included in our statistical analysis. Previous studies [*Anagnostopoulos et al.*, 1988; *Mason et al.*, 1996; *Meziane et al.*, 1998; *Desai et al.*, 2000] have shown that the occurrence of ions with $E \geq 50$ keV occur during specific conditions in the interplanetary medium, such as during CIR events and/or high solar wind speed. An example of an event that occurred in the presence of ambient ions in the interplanetary medium is depicted in Figure 9, which shows data from Wind acquired on 26 December 1999 between 0400 UT and 0500 UT. The solar wind conditions for this event were typical ($V_{SW} \sim 460$ km/s, $n_{SW} \sim 4\ cm^{-3}$ and $\beta \sim 0.5$). We found $\theta_{Bn}^{\mathrm{MV}} = 83°$, which is consistent with the model result $\theta_{Bn}^{\mathrm{BS}} = 79°$. Energetic ions

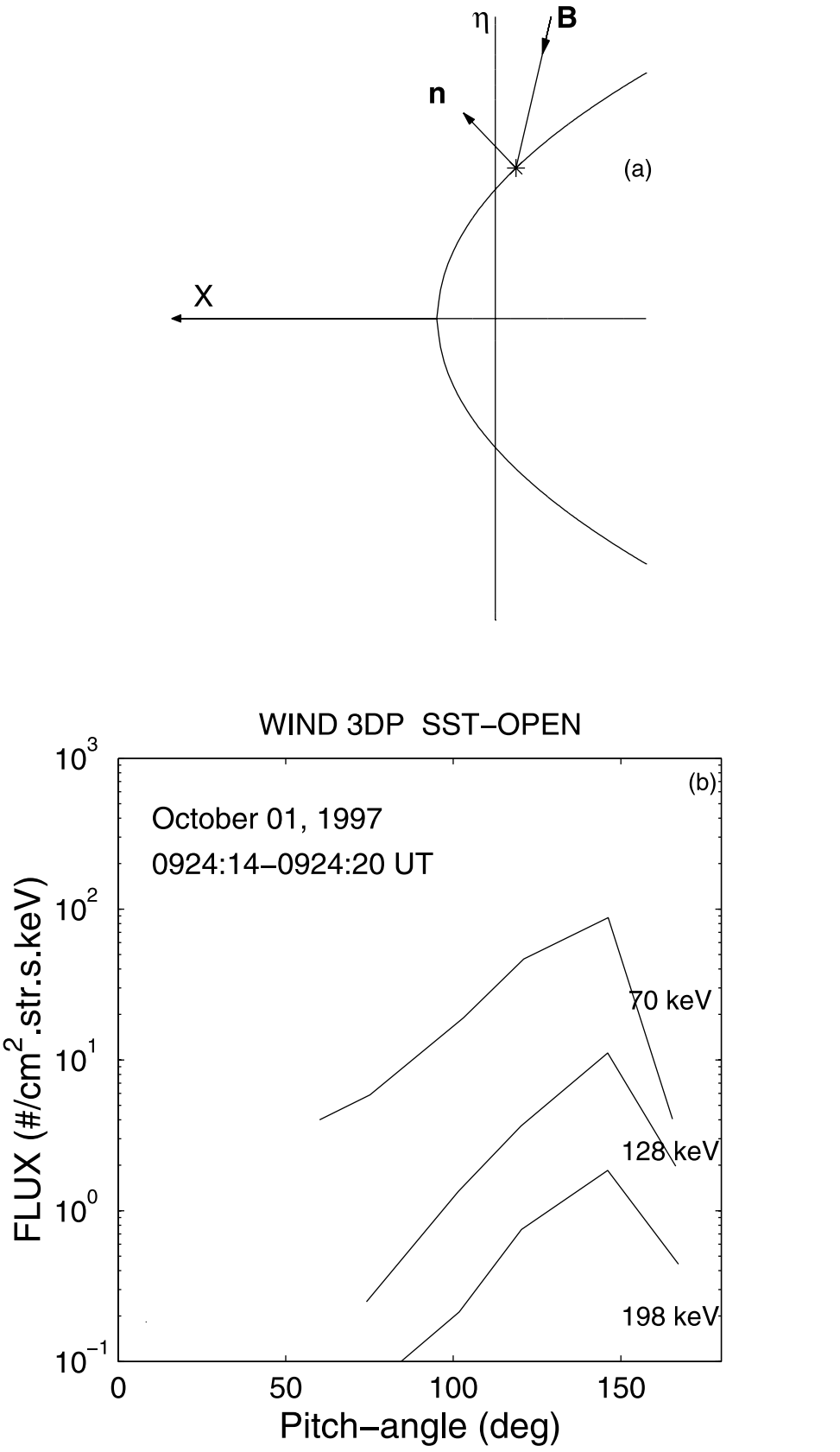

Figure 8. Top panel (a) indicates the shock geometry for the Wind bow shock crossing. Bottom panel (b) shows the particle pitch angle distribution for E = 70, 128 and 198 keV as registered just upstream of the bow shock on 1 October 1997 at 0924:14–0924:20 UT.

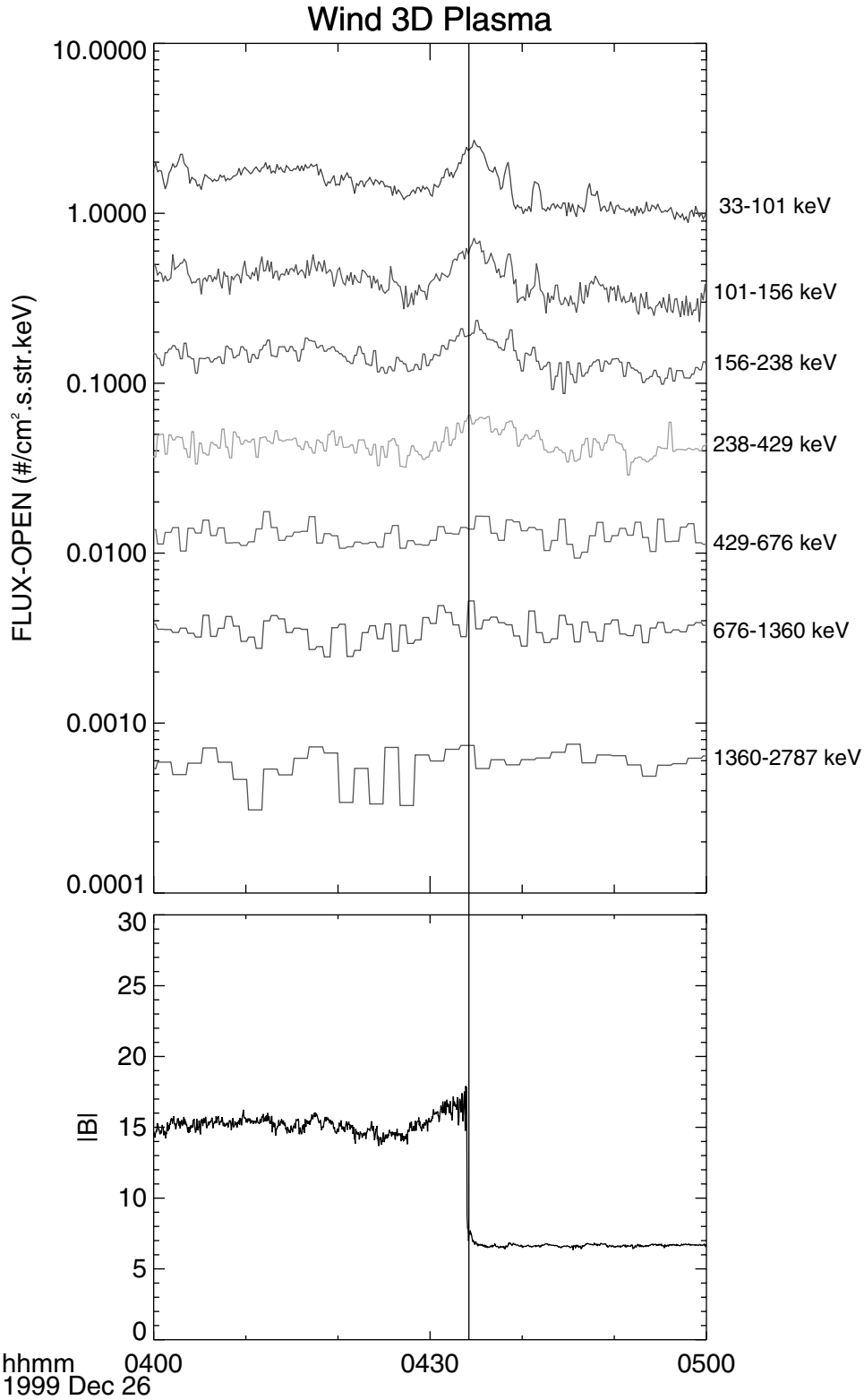

Figure 9. Same as in Figure 3 for 26 December 1999 between 0400 and 0500 UT.

with energies $E \geq 50$ keV of solar origin were present for two days prior to and during the bow shock crossing. Enhancements above the ambient ion flux levels are apparent just upstream of the shock ramp, which is at 0434:13 UT. Detailed examination of the pitch angle distribution function (not shown) revealed that the ions observed just upstream of the shock ramp are propagating away from the shock.

[18] In the detailed analysis each individual energetic ion event observed just upstream of the bow shock, we found that enhanced, upstream ion flux levels are almost always

due to ions propagating away from the shock. Very few events were found to be associated with ions moving toward the shock layer. Such events were not included in our study.

4. Statistical Results

[19] In this section we discuss the average properties of energetic ion flux levels as a function of geometry and energy. The events included in this study are associated with ions moving away from the shock. To better assess the processes responsible for the energetic ion enhancements, we separated the events into two categories. The first category consists of events that occur under quiet solar wind conditions, while the second consists of those events that are associated with a preexisting (seed) population of energetic particles with $E \geq 50$ KeV at 1 AU from the Sun. For comparison purposes, we averaged the omnidirectional fluxes according to θ_{Bn} bins 10° wide. It is important to note that the statistics for the CIR/SEP related events for low values of θ_{Bn} are quite poor. For this reason, we collapsed the lowest three bins when averaging the omnidirectional flux levels to increase statistics. The centroids of the averaging bins are $\langle\theta_{Bn}\rangle$ = 15°, 35°, 45°, 55°, 65°, 75°, and 85°. A histogram of events based on the averaging θ_{Bn} bins is given in Figure 10. Events were binned according to θ_{Bn} obtained via the minimum variance method. The shaded bars represent quiet solar wind conditions(with $V_{SW} \leq 480$), while the unshaded bars reflect the CIR/SEP related ion events. For the most part, our data set provides good coverage of all shock geometries.

4.1. Energy Spectrum

[20] Figure 11 shows the averaged upstream ion energy spectra corresponding to each $\langle\theta_{Bn}\rangle$ bin. The 21–33 keV ion measurement from PESA-H have been included in the spectra. The asterisks and open circle symbols represent events registered in absence and in the presence of ambient solar wind energetic ions with $E \geq 50$ keV, respectively. The average spectra corresponding to quiet solar wind conditions have an energy cutoff at $E \sim 330$ keV, at all values of θ_{Bn}. For $\theta_{Bn} \leq 40°$, the average energy spectra associated with CIR/SEP ions have a similar shape and a similar energy cutoff as found in the quiet solar wind spectra. However, at more oblique shock geometries ($\theta_{Bn} \geq 45°$), the spectra associated with ambient energetic ions have a high-energy tail which extends up to ~2 MeV. In addition, the slope of the high-energy tail tends to decrease with increasing values of θ_{Bn}. The dramatic differences between the properties of the CIR/SEP related spectra sampled at quasi-perpendicular shock crossings and the properties of those spectra sampled at quasi-parallel shock crossings is an indication of different mechanisms operating at these disparate shock geometrical regimes. We interpret the high-energy tail in CIR/SEP related spectra to be the result of diffusion free shock drift acceleration of a seed population of energetic ions (see discussion below in section 5.2). The absence of a high-energy component in the ambient related energy spectra depicted in the $\langle\theta_{Bn}\rangle$ = 55° panel is likely to be an artifact of the biases associated with the relatively low number of events observed at these transitional shock geometries, coupled with the uncertainties associated with the shock geometry determination. The presence of a high-energy component in the CIR/SEP related energy spectra depicted in the $\langle\theta_{Bn}\rangle$ = 45° panel is probably due to errors in the determination of the local shock geometry. A closer examination of events responsible for the "soft" high-energy spectra in the $\langle\theta_{Bn}\rangle$ = 45° panel revealed that those events had θ_{Bn}^{MV} near 50°, and given the uncertainties in θ_{Bn}^{MV}, these events are consistent with more quasi-perpendicular shock geometries.

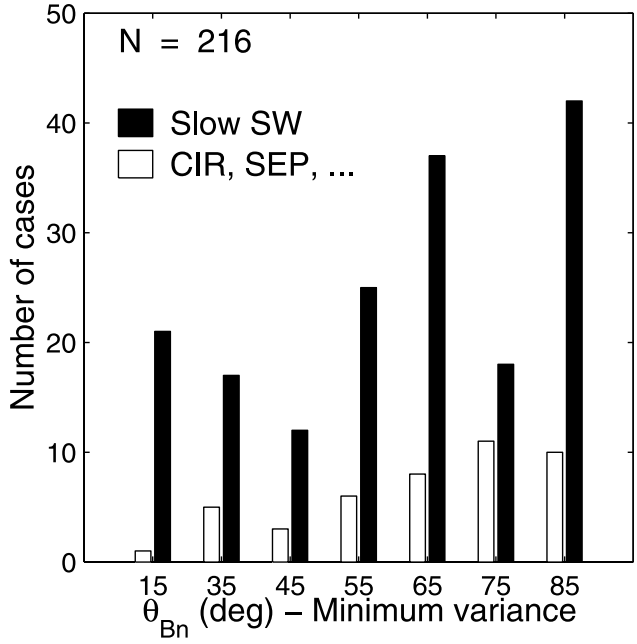

Figure 10. Histogram for θ_{Bn} angle as computed using the minimum variance analysis. Quit solar wind conditions cases have been separated from those obtained during the presence of ambient energetic particles.

4.2. Flux Profile Versus θ_{Bn}

[21] In this section we examine the relationship between the averaged upstream ion intensity and shock geometry. The panels given in Figure 12 show the variation of the averaged ion differential flux as a function of θ_{Bn} for each energy channel. The asterisks and open circles represent events associated with quiet interplanetary conditions and events that occurred in the presence of ambient energetic particles, respectively. The flux profiles depicted in each panel of Figure 12 are given in arbitrary units. Given the error bars, it appears that the ion flux levels associated with typical interplanetary conditions, for the most part, do not depend on θ_{Bn}. No significant ion fluxes associated with typical interplanetary conditions were observed at energies $E \geq 552$ keV. This is merely a reflection of the energy cutoff in the spectrum discussed in the previous section. The flux profiles associated with ambient CIR/SEP energetic ions depicted in Figure 12 have a local maximum near parallel geometry ($\theta_{Bn} \leq 30°$) in the energy range between 70 keV and 334 keV. The flux profiles reach a local minimum near $\langle\theta_{Bn}\rangle \sim 55°$, and subsequently attain a local maximum at more quasi-perpendicular geometries. The drop in intensity near $\langle\theta_{Bn}\rangle \sim 55°$ is most obvious in the $E \geq 128$ keV channels. This local minimum marks the transition between

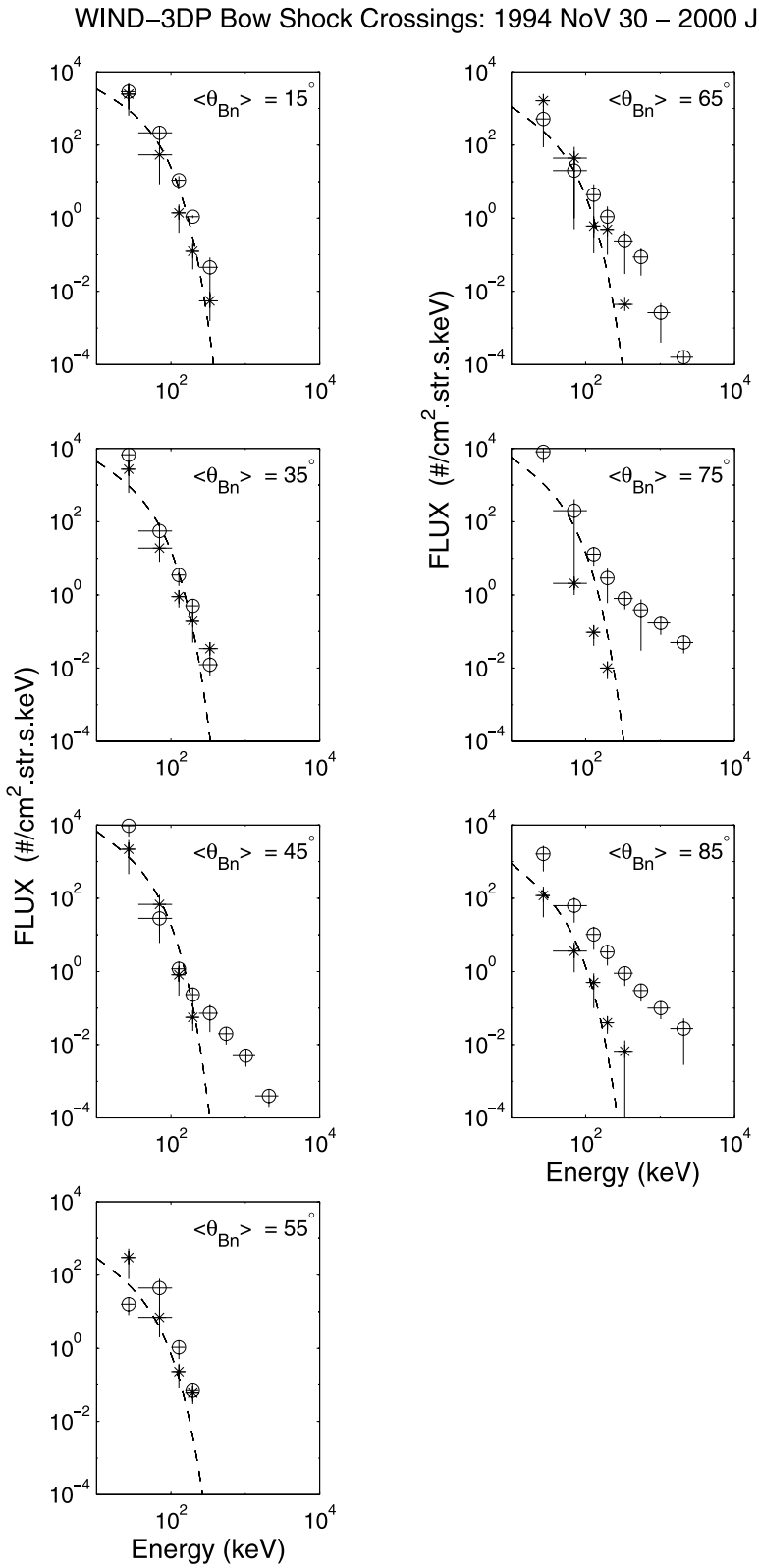

Figure 11. Energy spectrum for each θ_{Bn} angle range. The '*' and '○' symbols correspond to measurements registered during quiet solar wind conditions and in presence of ambient energetic particles, respectively.

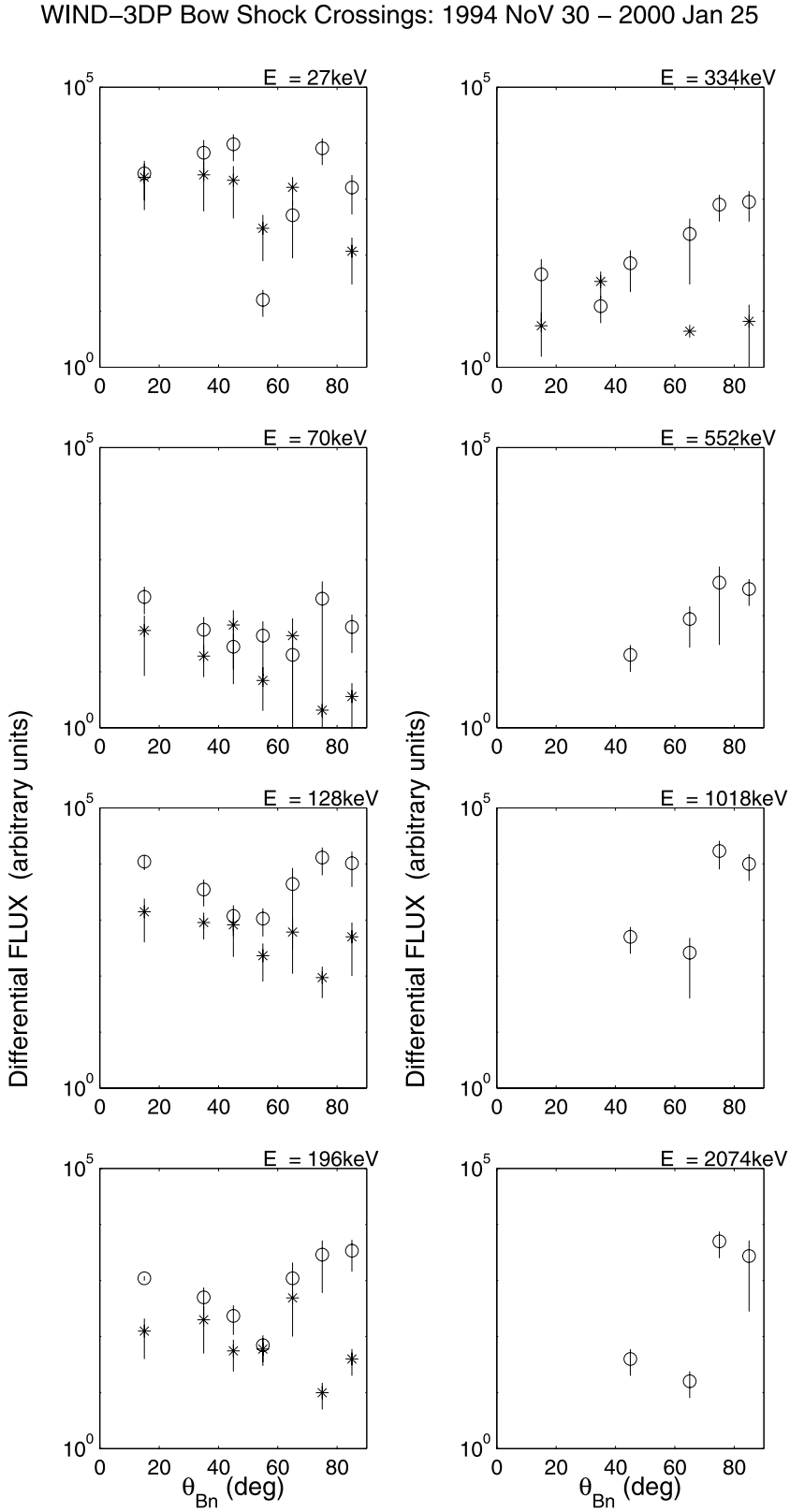

Figure 12. Particle fluxes versus θ_{Bn} angle for each energy range. The '*' and '○' symbols correspond to measurements registered during quiet solar wind conditions and in presence of ambient energetic particles respectively.

the different mechanisms that energizes ions at quasi-parallel and quasi-perpendicular shock geometries (see discussion belon in section 5). In addition, Figure 12 clearly shows that ions with energies $E \geq 550$ keV are observed only at quasi-perpendicular shock geometries. The averaged flux levels of these more energetic ions also tend to increase with increasing values of θ_{Bn}.

[22] The effects of the angle θ_{Bn} on the intensities have been first reported in case of energetic particles accelerated by interplanetary shocks associated with corotating interaction regions [*Tsurutani et al.*, 1982]. Using Pioneer 10 & 11 data, the statistical study carried out by Tsurutani et al. show that the maximum intensities of 0.5–1.8 MeV protons are observed at $\theta_{Bn} \sim 85°$. These results are consistent with the results of our study, suggesting that similar processes are acting at both interplanetary shocks associated with CIRs and the terrestrial bow shock to accelerate the particles at these quasi-perpendicular geometries. We suggest that the enhanced flux levels associated with a preexisting population of energetic ions can be explained in part by the SDA mechanism.

5. Discussion

[23] Our statistical results reveal the strong relationship between the energetic ion flux levels and shock geometry. These observational results place stringent constraints on the various theories/mechanisms proposed to explain the energetic ions emanating from the bow shock. Below we make quantitative comparisons between results of two candidate models and our observational results.

5.1. Quasi-parallel Shock Geometry

[24] As mentioned above, the energy spectra of the two classes of ion events are very similar for values of $\theta_{Bn} \leq 40°$. However, closer inspection reveals that the averaged omnidirectional flux levels associated with ambient energetic ions shown in Figure 12 have a local maximum in the 0°–30° bin. This peak in the flux level is likely to be an artifact of the Fermi acceleration mechanism, which is based on multiple reflections of particles between the shock and sufficiently large-amplitude, turbulent electromagnetic waves. Fermi acceleration is believed to be a plausible explanation for the flux enhancements near $\theta_{Bn} \sim 0°$ for two basic reasons. First, quasi-parallel regions of Earth's bow shock are associated with large amplitude, turbulent MHD. In particular, Ultra-low frequency (~30 seconds period) waves having substantial amplitude ($\Delta B/B \sim 1$) are often observed at quasi-parallel shocks. It is believed that these ULF waves are excited by field-aligned ion beams accelerated at quasi-perpendicular and oblique shocks. The excited waves in turn scatter the ion beam particles in pitch angle. During this process, the waves continue to grow and in the same time are convected toward quasi-parallel shock region [see review, *Thomsen*, 1985]. Magnetic field measurements from ISEE 2 have shown that the low-frequency turbulence level increases, on average, with distance from the ion foreshock boundary along X_{GSE}-axis [*Bavassano-Cattaneo et al.*, 1983]. Also, previous studies have shown that the energy-density associated with upstream particles increases with the magnetic turbulence level [e.g., *Trattner et al.*, 1994].

[25] The second reason behind maximum particle fluxes can be attributed to solar wind convection of particles toward the quasi-parallel region. Ions having small parallel velocities cannot escape upstream and must therefore be convected back toward the shock. These particles tend to accumulate at more quasi-parallel geometries of the terrestrial bow shock. Thus the increased fluxes near $\theta_{Bn} \sim 0°$ found in our observations may arise by virtue of the fact that there exists a larger seed population at these geometries.

[26] The energy spectra show an energy cutoff at $E \sim 200–330$ keV in the case where $\theta_{Bn} \leq 40°$, in agreement with previously published studies [*Ipavich et al.*, 1981; *Bonifazi and Moreno*, 1981; *Scholer*, 1990]. The energy spectra, including the cutoff in energy reported in this paper, places important constraints on the mechanism or mechanisms responsible for these energetic ions. The energy spectra result from a balance between the shock compression ratio, the typical injection rate at the shock, and particle backscatter by MHD turbulence in the quasi-parallel shock region.

[27] The theory of ion diffusive shock acceleration reported earlier by *Lee* [1982] and recently revisited by [*Gordon et al.*, 1999] is based on diffusive processes associated with the MHD waves and has been proposed to explain the signatures of energetic particles at quasi-parallel geometries. *Lee* [1982], predicted the energy-spectrum for any given distance from the shock using typical upstream conditions for a quasi-parallel geometry including the wave power spectrum. In order to compare with Lee's model, we determined the downstream to upstream compression ratio r using the Rankine-Hugoniot conservation relations for each bow shock crossing and using upstream plasma and magnetic field parameters (see section 4.3). The variation of r versus θ_{Bn} is plotted in the top panel of Figure 13. The obtained result is consistent with previous study on compression at the bow shock [*Argo et al.*, 1967]. Taking errors into account, both classes of events (with or without ambient energetic particles) yielded similar values of r for a given θ_{Bn}. The resulting central values of the compression ratio r at the shock are used to determine the ion energy spectrum for each $\langle\theta_{Bn}\rangle$, as predicted by Lee's theory. The predicted spectra are represented by the dashed curves on Figure 11. As far as normalization is concerned, the differential flux for ~27 keV protons at the shock has been taken equal to the observed values obtained in the present study. These values are 2.7×10^3 and 4.7×10^3 (protons/$cm^2.s.str.keV$) for $\langle\theta_{Bn}\rangle = 15°$ and 35° respectively. These values used are very similar to those reported by [*Ipavich et al.*, 1981] 4×10^3 (protons/$cm^2.s.str.keV$). It is clear that the agreement between the observations and Lee's theoretical model is good for $\theta_{Bn} \leq 40°$. For $\theta_{Bn} > 60°$, Lee's model clearly breaks down for events observed in presence of preexisting energetic particles. In absence of ambient energetic particles, there is partial agreement at quasi-perpendicular geometry.

[28] The comparison between the observations presented here and Lee's model supports the hypothesis that ion acceleration is likely to occur near the shock front irrespective of the source of the injected ions (or seed population). Recent ion composition studies of upstream ion events strengthen the hypothesis that the main source of the seed particles is located upstream [*Desai et al.*, 2000]. The possibility that the incoming thermal solar wind could be accelerated to ~100 keV has been investigated by *Ellison*

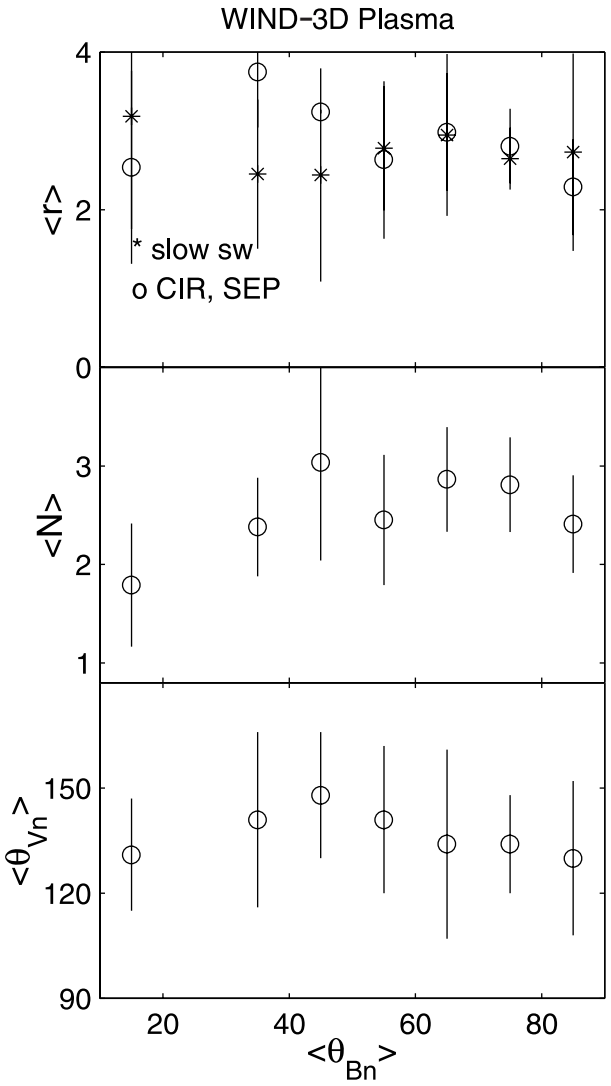

Figure 13. From bottom top panels, the θ_{Vn} angle between the upstream flow direction and the local bow shock normal, the cross-shock jump in magnetic field $N = B_2/B_1$, and the shock compression ratio r (see text) are plotted versus $\langle\theta_{Bn}\rangle$, respectively.

et al. [1990]. The study concludes that the shock-heated incoming ions are accelerated in the turbulent quasi-parallel region and recross the bow shock; a scenario consistent with simulation results. The flux profile as a function of θ_{Bn} would indicate that this process is statistically efficient for nearly parallel shock geometries ($\theta_{Bn} \sim 0°$), where the level of electromagnetic wave turbulence is optimum. Finally, the agreement between the observations and the shock-diffusive model reported by Lee does not, necessarily, rule out the possibility that particles may have a magnetospheric origin. The present results would then indicate that the intensity of upstream escaping energetic ions is maximum at for quasi-parallel shock geometries.

5.2. Quasi-perpendicular Shock Geometry

[29] The shock drift acceleration (SDA) mechanism is often considered to be the dominant acceleration process at quasi-perpendicular shock geometries [*Armstrong et al.*, 1985; *Forman and Webb*, 1985]. The theoretical predictions of the model based on the SDA mechanism of ion acceleration have been outlined in the paper by *Decker* [1988], where the shock is assumed to be laminar. The model developed by *Decker* [1988] assumes that the gyrophase averaged magnetic moment is conserved [*Pesses*, 1981; *Whipple et al.*, 1986]. This approximation stems from the conservation of the flux of angular momentum along particle trajectories and is a valid approximation in the asymptotic upstream and downstream states of perpendicular or nearly perpendicular shocks ($70° \leq \theta_{Bn} \leq 90°$). In his SDA model, *Decker* [1988] dealt with both reflected ions and ions transmitted from the downstream into the upstream side of the shock. According to *Decker* [1988], the ratio of the incident particle energy T_i to the postencounter particle energy T in the case of reflection is given by

$$\frac{T_i}{T} = 1 + 4\eta(\eta - \mu). \tag{1}$$

In the case of particles escaping from downstream to upstream, the expression takes the form

$$\frac{T_i}{T} = 1 + (1 + f^2)\eta^2 - 2\eta[\mu - f\sqrt{1 + \eta^2 - 2\eta\mu - N(1 - \mu^2)}]. \tag{2}$$

In the above equations μ is the cosine of the postencounter particle pitch angle, N is the cross-shock magnetic field jump $N = B_2/B_1$, $\eta^2 = T_s/T$, and $f = N/r$, where r is the upstream to downstream normal flow speed ratio and $T_s = \frac{1}{2}m_p(V_{SW}\frac{\cos\theta_{Vn}}{\cos\theta_{Bn}})^2$, θ_{Vn} being the angle that the upstream bulk velocity makes with the local shock normal. The parameter T_i/T is expressed in the plasma rest frame of reference.

[30] For a given θ_{Bn}, the T_i/T ratio is completely determined if N, r and θ_{Vn} are known. For each $\langle\theta_{Bn}\rangle$, the average values of N, r and θ_{Vn} are obtained from observations. Because of a PESA-H analyzer saturation problem, the r ratio is deduced from the resolution of the Rankine-Hugoniot continuity equations for each bow shock crossing and by using upstream plasma and magnetic field values [*Tidman and Krall*, 1971].

[31] Figure 13 displays the averaged values of θ_{Vn}, N, and r for each $\langle\theta_{Bn}\rangle$ in the case where ambient energetic particles are present (r is plotted for both cases). On the basis of central average values, the θ_{Vn} angle varies weakly with $\langle\theta_{Bn}\rangle$. However, the averaged jump in magnetic field magnitude increases on average with increasing $\langle\theta_{Bn}\rangle$ as expected for fast-mode shocks. The T_i/T ratio being known, the energy spectrum is obtained assuming conservation of phase space density along particle orbits. Assuming the incident energy spectrum to be isotropic, we can show that the omnidirectional differential flux is:

$$j(T) = \frac{1}{2}\int_{\mu_1}^{\mu_2} d\mu j_i(T_i(T,\mu)) \tag{3}$$

with $\mu_1 = \eta$ and $\mu_2 = \mu_c$ for the reflected particles, whereas for the transmitted upstream particles $\mu_1 = \mu_c$ and $\mu_2 = 1$, with $\mu_c = (\eta + \sqrt{(N-1)(N-\eta^2)})/N$.

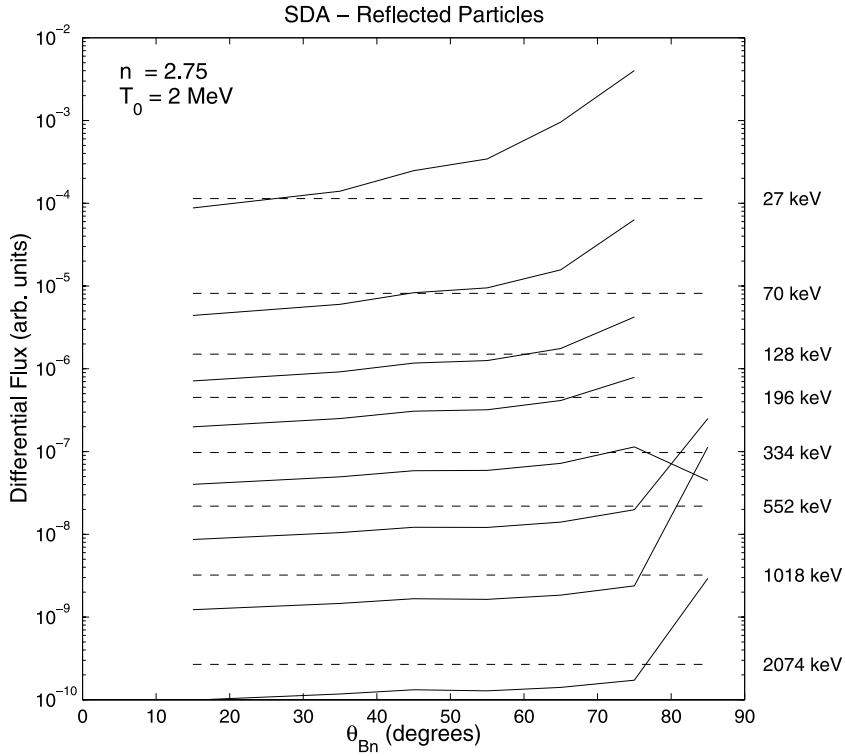

Figure 14. Each curve represents the omnidirectional differential flux as predicted by the SDA mechanism for reflected particles versus $\langle\theta_{Bn}\rangle$. The dashed line associated with each curve indicates the incoming flux level at the same energy.

[32] An initial energy spectrum profile j_i must be prescribed as input in order to compute the postencounter spectrum j. Using equation (3) we compute, for a fixed energy and for a given $\langle\theta_{Bn}\rangle$, the differential flux which we then compare with the incident differential flux at the same energy. When possible, the integral is computed analytically, otherwise it is done numerically. In the present development we only consider the case when ambient energetic particles are present. In this case, the question of the origin of the seed population (injection problem) does not arise. The thermal solar wind cannot account for the seed population for this mechanism to be sufficient to accelerate to very high energy. The SDA mechanism enables the acceleration of solar wind particles up to ~10 keV [*Terasawa*, 1979a, 1979b]. As indicated above the ambient energetic particles are accelerated by interplanetary shocks associated with CIR or/and SEP events. Studies conducted on these accelerated particle populations have been reported and the energy spectra are available in the literature. Recently, *Desai et al.* [1999] have reported that accelerated particles at CIRs give rise to an energy spectrum profile of the form (the normalization factor has been taken equal to 1):

$$j_i(T_i) = T_i^{-n}\exp(-T_i/T_0), \tag{4}$$

The spectral index n may vary from ~1 to ~3 in general, and the width $T_0 \sim 1-3$ MeV [*Desai et al.*, 1999]. The energy spectrum profiles associated with SEP events are power law types:

$$j_i(T_i) = T_i^{-\gamma}, \tag{5}$$

with $\gamma \sim 2.5 \pm 1$. The expression of $j_i(T_i)$ is used as an input in expression (3), and the postencounter energy spectrum is derived. We have performed calculations using the forms (4) and (5) which lead to qualitatively similar results. Below we only present results obtained using the form (5) of $j_i(T_i)$.

5.2.1. Reflection at Shock

[33] Figure 14 shows the predicted differential flux associated with reflected particles at the shock versus θ_{Bn}. We used $n = 2.25$ and $T_0 = 2$ MeV. Each solid curve represents predicted fluxes for a given energy T. The dashed curves indicate input flux levels $j_i(T)$. Below a critical θ_{cBn}, the SDA predicts flux levels that are depressed relative to the incident levels. Because the escaping accelerated ions have to overrun the shock, the critical θ_{cBn} value increases with energy as expected from the SDA mechanism [*Armstrong et al.*, 1985]. It is clear that the reflected flux at all energies is substantially higher than the initial flux level for the quasi-perpendicular geometry only. High-energy fluxes ($E \geq 550$ keV) arise when $\theta_{Bn} \geq 75°$ while low-energy fluxes, at energies $E \leq 198$ keV, are absent as expected from the SDA mechanism. Using other values of n and T_0 does not substantially affect the profiles plotted in Figure 14.

[34] The results of Figure 14 only partially explain the data shown on Figure 12. It is clear that the upstream events observed in the quasi-parallel shock region are not understood in terms of the SDA mechanism. On the other hand, the events associated with the quasi-perpendicular shock region seem to agree with the SDA model. The agreement between theory and observations is relatively good in the energy range between $E = 1$ MeV and $E = 2$ MeV. For $\theta_{Bn} \geq 75°$, the ion flux increases by about one order of magnitude

in the 1 to 2 MeV range in agreement with the observations. However, Figure 12 indicates that upstream fluxes higher than the incident flux are observed for $\theta_{Bn} \sim 45°$ and higher, which is not predicted by the diffusion-free SDA mechanism. We suspect the spread in parameter space (r, N, θ_{Vn}, n, T_0 and γ) to be at the origin of the discrepancy.

[35] These results agree with the study reported by *Freeman et al.* [2000] which used simulations and observations of energetic particles observed upstream of the bow shock. The study indicates that energetic particle (500 keV − 2 MeV) observed upstream of the quasi-parallel region originate in fact from the quasi-perpendicular shock region.

5.2.2. Escape From Downstream

[36] We have used equation (2) to compute the expected flux levels of shock accelerated particles escaping to the upstream side of the shock from the magnetosheath. We found that the intensity for $E \geq 70$ keV is less than the incident flux levels, regardless of the value of θ_{Bn}. This result excludes the hypothesis that the energetic particles may escape from downstream after being accelerated by an SDA mechanism.

6. Conclusion

[37] Most of bow shock associated ion spectra reported in previous studies did not address the impact of θ_{Bn} angle. We have conducted a statistical study of ion intensities measured just upstream of Earth's bow shock. In particular we examined the detailed relationship between averaged ion flux levels and shock geometry. By concentrating on upstream events relatively close to the shock layer, we are able to more clearly identify dependencies of the upstream ion flux levels on shock geometry than possible from previous studies. The events registered were separated into two classes: the first class consists of events which occurred during typical solar wind conditions, while the second class is composed of events associated with a preexisting solar wind energetic ion population. As one may expect, the properties of the ion intensities depend strongly on the source regions of the ions, whether they be from the quasi-perpendicular or quasi-parallel bow shock regions. We find that the energy spectrum of ion events associated with typical solar wind conditions and in absence of ambient energetic ions falls off sharply, having a cutoff at $E \sim 200-330$ keV, independent of θ_{Bn}. These observations provide important constraints for the various models proposed to explain the upstream energetic ion signatures. The shock-diffusive ion acceleration theory as reported by *Lee* [1982] provides a satisfactory explanation for energetic particles observed in quasi-parallel shock conditions. Ions with energies above 330 keV are always associated with a preexisting energetic ion population and they are observed to occur only at quasi-perpendicular bow shock geometries. These more energetic ion events appear to be the result of shock drift acceleration of the initial seed population of energetic ions at Earth's bow shock.

[38] **Acknowledgments.** Michel Blanc thanks both referees for their assistance in evaluating this paper.

References

Anagnostopoulos, G. C., E. T. Sarris, and S. M. Krimigis, Observational test of shock drift acceleration and Fermi acceleration on a seed particle population upstream of Earth's bow shock, *J. Geophys. Res.*, *93*, 5541, 1988.

Argo, H. V., J. R. Asbridge, S. J. Bame, A. J. Hundhausen, and I. B. Strong, Observations of solar wind plasma changes across the bow shock, *J. Geophys. Res.*, *72*, 1989, 1967.

Armstrong, T. P., M. E. Pesses, and R. B. Decker, Shock drift acceleration, in *Collisionless Shocks in the Heliosphere: A Tutorial Review*, *Geophys. Monogr. Ser.*, vol. 34, edited by R. G. Stone and B. Tsurutani, p. 271, AGU, Washington, D. C., 1985.

Bavassano-Cattaneo, M. B., C. Bonifazi, M. Dobrowolny, G. Moreno, and C. T. Russell, Distribution of MHD wave activity in the foreshock region and properties of backstreaming protons, *J. Geophys. Res.*, *88*, 9280, 1983.

Bonifazi, C., and G. Moreno, Reflected and diffuse ions backstreaming from the Earth's bow shock, 1, Basic properties, *J. Geophys. Res.*, *86*, 4397, 1981.

Cairns, I. H., D. H. Fairfield, R. R. Anderson, V. E. H. Carlton, K. I. Paularena, and A. J. Lazarus, Unusual locations of Earth's bow shock on September 24–25, 1987: Mach number effects, *J. Geophys. Res.*, *100*, 47, 1995.

Decker, R. B., Computer modeling of test particle acceleration at oblique shocks, *Space Sci. Rev.*, *48*, 195, 1988.

Desai, M. I., R. G. Marsden, T. R. Sanderson, D. Lario, E. C. Roelof, G. M. Simnett, J. T. Gosling, A. Balogh, and R. J. Forsyth, Energy spectra of 50 keV to 20 MeV protons accelerated at corotating interaction regions at Ulysses, *J. Geophys. Res.*, *104*, 6705, 1999.

Desai, M. I., G. M. Mason, J. R. Dwyer, J. E. Mazur, T. T. von Rosenvinge, and R. P. Lepping, Characteristics of energetic ($\geq$ 30 keV/nucleon) ions observed by the Wind/STEP instrument upstream of the Earth's bow shock, *J. Geophys. Res.*, *105*, 61, 2000.

Edmiston, J. P., C. F. Kennel, and D. Eichler, Escape of heated ions upstream of quasi-parallel shocks, *Geophys. Res. Lett.*, *9*, 531, 1982.

Ellison, D. C., E. Mobius, and G. Paschmann, Particle injection and acceleration at Earth's bow shock: Comparison of upstream and downstream events, *Astrophys. J.*, *352*, 376, 1990.

Forman, M. A., and G. M. Webb, Acceleration of energetic particles, in *Collisionless Shocks in the Heliosphere: A Tutorial Review*, *Geophys. Monogr. Ser.*, vol. 34, edited by R. G. Stone and B. Tsurutani, p. 91, AGU, Washington, D. C., 1985.

Freeman, T. J., and G. K. Parks, Fermi acceleration of suprathermal solar wind oxygen ions, *J. Geophys. Res.*, *105*, 15,715, 2000.

Freeman, T. J., D. E. Larson, R. P. Lin, K. Meziane, G. K. Parks, Characteristics of MeV upstream ion bursts observed by Wind, in *Acceleration and Transport of Energetic Particles Observed in the Heliosphere: ACE-2000 Symposium, Indian Wells, California, 5–8 January 2000*, edited by R. A. Mewaldt et al., AIP Conf. Proc., *528*, 286, 2000.

Fuselier, S. A., Suprathermal ions upstream and downstream from the earth's bow shock, in *Solar Wind Source of Magnetospheric Ultra-Low Frequency Waves*, *Geophys. Monogr. Ser.*, vol. 81, edited by M. Engebretson, M. Takahashi, and M. Scholer, p. 107, AGU, Washington, D. C., 1994.

Gordon, B. E., A. M. Lee, E. Möbius, and K. J. Trattner, Coupled hydromagnetic wave excitation and ion acceleration at interplanetary traveling shocks and Earth's bow shock revisited, *J. Geophys. Res.*, *104*, 28,263, 1999.

Gosling, J. T., M. F. Thomsen, S. J. Bame, W. C. Feldman, G. Paschmann, and N. Sckopke, Evidence for specularly reflected ions upstream from the quasi-parallel bow shock, *Geophys. Res. Lett.*, *9*, 1333, 1982.

Greenstadt, E. W., C. T. Russell, and M. Hoppe, Magnetic field orientation and suprathermal ion streams in the Earth's foreshock, *J. Geophys. Res.*, *85*, 3473, 1980.

Ipavich, F. M., A. B. Galvin, G. Gloeckler, M. Scholer, and D. Hovestadt, A statistical survey of ions observed upstream of the Earth's bow shock: Energy spectra, composition, and spatial variation, *J. Geophys. Res.*, *86*, 4337, 1981.

Lee, M. A., Coupled hydromagnetic wave excitation and ion acceleration upstream of the Earth's bow shock, *J. Geophys. Res.*, *87*, 5063, 1982.

Lepping, R. P., et al., The Wind magnetic field experiment, *Space Sci. Rev.*, *71*, 207, 1995.

Lin, R. P., et al., A three-dimensional plasma and energetic particle investigation for the Wind spacecraft, *Space Sci. Rev.*, *71*, 125, 1995.

Lin, R. P., C.-I. Meng, and K. A. Anderson, 30- to 100-keV protons upstream from the Earth's bow shock, *J. Geophys. Res.*, *79*, 489, 1974.

Mason, G. M., J. E. Mazur, and T. T. von Rosenvinge, Energetic heavy ions observed upstream of the Earth's bow shock by the STEP/EPACT instrument on Wind, *Geophys. Res. Lett.*, *23*, 1231, 1996.

Meziane, K., R. P. Lin, R. Campbell, D. E. Larson, G. K. Parks, G. M. Mason, J. R. Dwyer, and R. P. Lepping, Property survey of 2 MeV ions in the Earth's bow shock, *Eos Trans. AGU*, *79*(17), Spring Meet. Suppl., S311, 1998.

Meziane, K., R. P. Lin, G. K. Parks, D. E. Larson, S. D. Bale, G. M. Mason, J. R. Dwyer, and R. P. Lepping, Evidence for acceleration of ions to ~1 MeV by adiabatic-like reflection at the quasi-perpendicular Earth's bow shock, *Geophys. Res. Lett.*, *26*, 2925, 1999.

Mitchell, D. G., and E. C. Roelof, Dependence of 50 keV upstream ion events at IMP 7 and 8 upon magnetic field bow shock geometry, *J. Geophys. Res.*, *88*, 5623, 1983.

Paschmann, G., N. Sckopke, I. Papamastorakis, J. R. Asbridge, S. J. Bame, and J. T. Gosling, Characteristics of reflected and diffuse ions upstream from the Earth's bow shock, *J. Geophys. Res.*, *86*, 4355, 1981.

Pesses, M. E., On the conservation of the first adiabatic invariant in perpendicular shocks, *Geophys. Res.*, *86*, 150, 1981.

Sarris, E. T., G. C. Anagnostopoulos, and S. M. Krimigis, Simultaneous measurements of energetic ion (≥50 keV) and electron (≥220 keV) activity of Earth's bow shock and inside the plasma sheet: Magnetospheric source for the November 3 and December 3, 1977 upstream events, *J. Geophys. Res.*, *92*, 12,083, 1987.

Scholer, M., Diffuse ions at quasi-parallel collisionless parallel shocks: Simulations, *Geophys. Res. Lett.*, *17*, 1821, 1990.

Scholer, M., F. M. Ipavich, G. Gloeckler, and D. Hovestadt, Conditions for acceleration of energetic ions ≥30 keV associated with the Earth's bow shock, *J. Geophys. Res.*, *85*, 4602, 1980.

Skoug, R. M., et al., Upstream and magnetosheath energetic ions with energies to ~2 MeV, *Geophys. Res. Lett.*, *23*, 1223, 1996.

Sonnerup, B. U. Ö., and L. J. Cahill, Magnetopause structure and attitude from Explorer 12 observations, *J. Geophys. Res.*, *72*, 171, 1967.

Terasawa, T., Energy spectrum and pitch angle distribution of particles reflected by MHD shock waves of fast mode, *Planet. Space Sci.*, *27*, 193, 1979a.

Terasawa, T., Origin of 30–100 keV protons observed in the upstream region of the Earth's bow shock, *Planet. Space Sci.*, *27*, 365, 1979b.

Terasawa, T., Energy spectrum of ions accelerated through Fermi process at the terrestrial bow shock, *J. Geophys. Res.*, *86*, 7595, 1981.

Thomsen, M. F., Upstream suprathermal ions, in *Collisionless Shocks in the Heliosphere: A Tutorial Review*, *Geophys. Monogr. Ser.*, vol. 34, edited by R. G. Stone and B. Tsurutani, p. 253, AGU, Washington, D. C., 1985.

Tidman, D. A., N. A. Krall, *Shock Waves in Collisionless Plasmas*, Wiley-Interscience, New York, 1971.

Trattner, K. J., E. Möbius, M. Scholer, B. Klecker, M. Hilchenbach, and H. Lühr, Statistical analysis of diffuse ion events upstream of the Earth's bow shock, *J. Geophys. Res.*, *99*, 13,389, 1994.

Tsurutani, B. T., E. J. Smith, K. R. Pyle, and J. A. Simpson, Energetic protons accelerated at corotating shocks: Pioneer 10 and 11 observations from 1 to 6 AU, *J. Geophys. Res.*, *87*, 7389, 1982.

Viñas, A. F., and J. D. Scudder, Fast and optimal solution to the "Rankine-Hugoniot Problem," *J. Geophys. Res.*, *91*, 39, 1986.

Whipple, E. C., T. G. Northrop, and T. J. Birmingham, Adiabatic theory in regions of strong field gradients, *J. Geophys. Res.*, *91*, 4149, 1986.

Zhang, Y., H. Matsumoto, H. Kojima, and Y. Omura, Extremely intense whistler mode waves near the bow shock: Geotail observations, *J. Geophys. Res.*, *104*, 449, 1999.

A. M. Hamza and K. Meziane, Physics Department, University of New Brunswick, Fredericton, New Brunswick, Canada E3B 5A3.

A. J. Hull and R. P. Lin, Space Sciences Laboratory, University of California, Berkeley, CA 94720, USA.